



Research Paper

Sustainable syngas and H₂ from a zootechnical waste: an investigation on fluidized bed gasification of cattle manureFrancesco Miccio^{a,*}, Izabella Maj^b, Lucrezia Polchri^a, Annalisa Natali Murri^a^a Institute of Science, Technology and Sustainability for Ceramics, Italian National Research Council, via Granarolo 64, 84018 Faenza, Italy^b Department of Power Engineering and Turbomachinery, Faculty of Energy and Environmental Engineering, Silesian University of Technology, 44-100 Gliwice, Poland

ARTICLE INFO

Keywords:

Gasification
Biomass
Cattle manure
Fluidized bed
Hydrogen
Ash

ABSTRACT

Cattle manure (CM) is a zootechnical waste no longer desired for direct land application. Therefore, alternative methods of disposal must be developed, especially in countries with high production of dairy products and meat. Fluidized bed gasification allows for the safe utilization of manure together with the recovery of energy in the form of syngas. In the presented research, CM was subjected to fluidized bed gasification in CO₂ and O₂ atmospheres at T = 850 °C. Different CO₂ levels (Y_{CO2} = 0.10, 0.20, and 0.30) or equivalence ratios for O₂ (χ = 0.3, 0.4, and 0.5) were used during gasification tests at laboratory scale. For the CO₂ atmosphere, the gas yields of H₂, CH₄, and CO were the highest at Y_{CO2} = 0.30 with a conversion degree of 73.7 % and maximum cold gas efficiency of 83.1 %. For O₂ atmosphere, the conversion degree of 86.4 % and maximum cold gas efficiency of 60.0 % were achieved at lowest equivalence ratio (χ = 0.3). An exploratory test confirmed the advantage of using a catalytic bed material (dolomite) compared to an inert one (quartzite). The presence of dolomite led to increased levels of H₂ and CH₄. Tar yield and characteristics for CM and reference beech wood (BW) were similar, although a slightly larger amount was appreciated for CM.

1. Introduction

Thermal conversion of biomass and waste brings both environmental and socioeconomic benefits in the transition to a more sustainable energy scenario. It provides energy flexibility and reduces greenhouse gas (GHG) emissions by replacing fossil fuels, thus aiding climate change mitigation (Poornima et al., 2024; Taifouris and Martín, 2023). It also supports rural development, especially in agricultural regions rich in biomass resources (Akter et al., 2024; Ersoy and Ugurlu, 2024).

With rising global meat and dairy consumption, annual animal manure production is increasing. An adult cow produces 10.0–26.0 tons of waste per year, depending on the bedding system used (Polish Council of Ministers, 2020). Animal litter is no longer favorable for land spreading due to concerns of uncontrolled greenhouse gases (GHG) emissions, water bodies eutrophication, the danger of pathogens spread, and antibiotics contamination (Al Zahra et al., 2024; Chen and Jiang, 2014; Moffo et al., 2021). Thermal treatment offers a solution by converting this low-value waste into energy-rich products like syngas, enhancing sustainability and energy security (Al-Rumaihi et al., 2023; Cai et al., 2021).

Gasification is one of the common methods for the thermo-chemical

conversion of waste and biomass, owing to the advantages of producing synthetic gas for further use, e.g. in internal combustion engines (Gabbrielli et al., 2016) or biofuels production (Molino et al., 2018). Abundant literature is available on the gasification of wood and agro biomass, while animal litter is far less recognized. Some vital differences exist in the properties and elemental composition of animal litter compared to conventional biomass, including lower heating value, higher ash content, and higher nitrogen content (Font-Palma, 2019; Maj, 2022). These differences are a reason for different behavior during the gasification and pyrolysis of animal litter, which has not been studied enough. Some studies focusing on poultry litter (PL) can be found, most of them involving fixed and fluidized bed reactors. Air and air–steam PL gasification in a laboratory-scale fluidized bed reactor using silica sand as the bed material, achieved the optimal carbon conversion, gas yield, heating value, and cold gas efficiency at moderately high temperature, i. e. 800 °C (Pandey et al., 2016). Another research (Kwon et al., 2019) investigated CO₂ as a reactive gas medium in the conversion of PL, observing a catalytic effect due to the high mineral contents. The CO₂ environment favored the generation of CO, which was ascribed to the homogenous reactions between the liquid phase of pyrogenic products and CO₂. The pyrolysis and gasification tests of chicken manure was investigated using different atmospheres and temperatures ranging

* Corresponding author.

E-mail address: francesco.miccio@cnr.it (F. Miccio).

Nomenclature		Greek symbols	
C_{conv}	carbon conversion, –	Ξ	conversion degree, –
E	activation energy, kJ/mol	Φ	tar yield, mg/g
m_{fuel}	mass of fuel, g	X	equivalence ratio, –
m_{tar}	mass of tar, g	Ψ	gas yield, mmol/g
Q	volumetric flow rate, mL/min	Acronyms	
R	universal constant of gases, J/(mol·K)	AU	atomic units
S	slope of conversion rate maxima	BW	beech wood
t	time, s	CGE	cold gas efficiency, %
T	temperature, °C	CM	cattle manure
U	fluidization velocity, m/s	GC	gas chromatography
U_{mf}	minimum fluidization velocity, m/s	LHV _{fuel}	low heating value of fuel, MJ/kg
X_C	carbon fraction in fuel, –	LHV _{gas}	low heating value of gas, MJ/m ³
Y	volumetric fraction, %	TG	thermo-gravimetry

between 600 and 1000 °C and the gasification with CO₂ and steam was found to result in syngas with the highest energy yield (Hussein et al., 2017). A subsequent study (Burra et al., 2016) investigated syngas evolutionary behavior during chicken manure pyrolysis and air gasification yielding a high concentration of methane as a by-product from the thermal cracking of hydrocarbons.

Contrary to poultry litter, cattle manure (CM) gasification is poorly explored and has only recently appeared in the literature. A limited number of experimental papers can be found, such as cow dung conversion for hydrogen production by coupling high-temperature pyrolysis and water vapor gasification in a tube furnace (Zhu et al., 2022). In similar research, CM was subjected to gasification coupled with inline co-steam reforming (Kong et al., 2023). Co-gasification of cow manure and bituminous coal blends at 800–1100 °C using a thermogravimetric analyzer was also performed (Ma et al., 2020). A detailed study reports on the gasification of cattle dung in a small-scale tubular furnace (Ashraf et al., 2022), performed at varying air–fuel equivalence ratios ER = 0.21–0.3. The optimal fractions of H₂ (13.26 ± 0.95 %), CO (14.39 ± 1.2 %), and CH₄ (2.15 ± 0.5 %) were achieved at 800 °C and ER = 0.26. The HHV of syngas was 4.89 ± 0.4 MJ/Nm³ at optimal process conditions. Based on the solid residue and thermal conversion efficiencies, 82.67 ± 1.2 % of biomass was converted to syngas, and 66.70 ± 2 % of biomass energy was extracted through gasification. In a comparative investigation between gasification and pyrolysis of CM (Constantinescu et al., 2024), high concentration of H₂ (up to 25 % vol.) was reported during transient tests in fixed bed under CO₂ atmosphere at temperature over 800 °C. The air gasification of animal manure can be exothermic, which means that the process can be sustained without external heating (Selim et al., 2020). The comparison of the performance of CO₂ and O₂ as gasifying agents in the fluidized bed reactor is rarely addressed in previous works, despite allowing for a more accurate assessment of how the gasifying medium influences gas yields. Also, the solid residues and produced tar are rarely investigated, which are important in terms of environmental and practical dimensions, especially in the context of waste management and potential utilization of gasification residues.

In this study, CM gasification in fluidized bed is proposed and experimentally investigated for the first time at laboratory scale by single pellet feeding. A comparative and holistic analysis of CO₂ and O₂ gasification was conducted, with main focus on yields of valuable species and syngas characteristics. The effect of a catalytic bed, the tar formation and ashes exploitation have been also addressed in the study. The findings provide fundamental and applied insights into CM gasification, offering valuable guidance for the design and optimization of gasifiers tailored more generally to high-ash, low-energy-content waste feedstocks.

2. Materials and methods

2.1. Fuels

In this study, dry CM collected from Polish farms was used as the primary feedstock. For comparative gasification experiments, a reference biomass, i.e. beech wood chips (BW), was utilized. Before the experiments, the manure was dried in oven at 105 °C and stored in closed bottles. Both fuels were pelletized to ensure stable feeding into the reactor. The raw CM and BW are depicted in Fig. 1a-b, while their respective pelletized forms are shown in Fig. 1c-d.

The properties of the tested fuels are reported in Table 1. The elemental analysis was conducted according to ISO 16948:2015–07 (C, H, N) and ISO 16994:2016–10 (Cl, S). Ash content in fuels was determined according to ISO 18122:2016–01, lower and higher calorific values according to ISO 18125:2017–07. The elemental analysis of ashes in oxide form was conducted by inductively coupled plasma–optical emission spectroscopy (ICP-OES) and ash fusion temperatures were determined in oxidizing conditions according to ISO 21404:2020–08. Both fuels display large volatile content, over 70 %wt on a dry ash-free basis. CM is characterized by higher ash content compared to BW, caused by its origin but also by the presence of impurities from the environment, such as SiO₂. CM contains a small amount of sulfur and a rather high content of nitrogen, owing to its zootechnic origin. CM is heterogeneous in origin and its composition may vary depending on location and season; similar analytical data are reported in the literature (Constantinescu et al., 2024).

Both feedstocks were pelletized using a linear press (Nannetti, Faenza, Italy) at room temperature within a 10 mm circular mold, applying a pressure of 10 MPa. The resulting pellets are shown in Fig. 1c-d. The pelletization facilitates reliable feeding into the gasification reactor, as the produced pellets possess a well-controlled size and a mass of 0.50 ± 0.02 g. Notably, no binding agents were required for the pelletization of either CM or BW. The pelletized CM exhibits a higher mass density than BW due to its greater ash content. Despite its higher ash content and lower heating value, CM also demonstrates a higher energy density compared to BW. The compressive strength of the pellets was measured in triplicate using a Z050 universal testing machine (Zwick-Roell, Ulm, Germany), as this parameter significantly impacts both storage stability and feeding efficiency.

2.2. Thermogravimetric apparatus

To determine the conversion rates and activation energies of CM and BW thermogravimetric (TG) tests have been carried out. The tests have been performed on a STA 449C Jupiter thermogravimetric balance (NETZSCH, Selb, Germany). The biomass sample of around 50 mg was

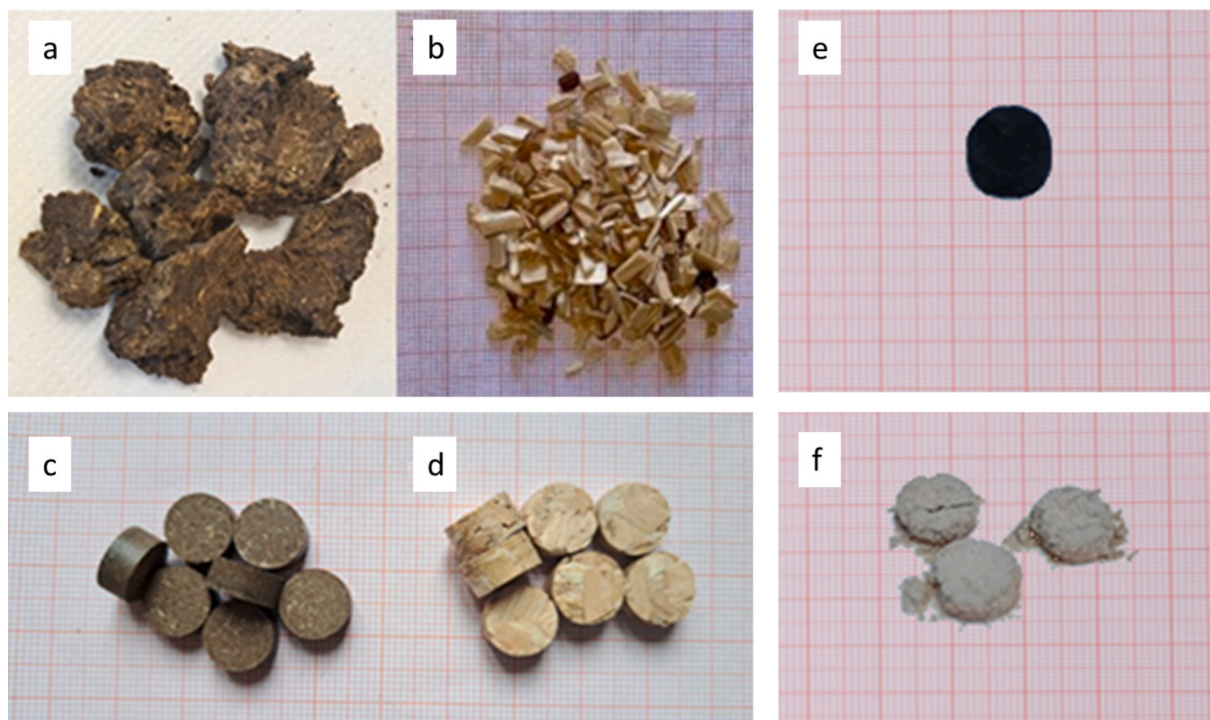


Fig. 1. Photographs of a) CM, b) BW, c) CM pellets, d) BW pellets, e) CM char from gasification, f) CM ash after full conversion.

subject to inert (N_2) and oxidizing atmosphere (N_2/CO_2) with a flow rate of 90 mL/min and a heating rate of 20 K/min up to 850 °C.

2.3. Experimental fluidization plant

A laboratory fluidized bed plant was used for batch gasification tests. The tests were conducted in an atmosphere containing O_2 , CO_2 , or N_2 . First, the experimental runs were carried out in oxygen atmospheres with equivalence ratios $\chi = 0.3, 0.4,$ and 0.5 for CM and $\chi = 0.5$ for BW. Then the CO_2 gasification was carried out in CO_2 volumetric fractions $Y_{CO_2} = 0.10, 0.20,$ and 0.30 for CM and $Y_{CO_2} = 0.10$ for BW. Pure nitrogen atmosphere, i.e. pyrolysis, was tested for CM. All tests have been carried out at temperature $T = 850$ °C and atmospheric pressure.

The fluidization column consisted of an AISI-316 stainless steel tube with an internal diameter of 29 mm and a height of 500 mm, as illustrated in Fig. 2. The gas was distributed from the bottom of the column through a stainless-steel mesh pack. The top end of the column was designed for fuel feeding and gas sampling. A K-type thermocouple was installed from the bottom side in contact with the mesh pack to control the reactor temperature. The temperature difference with the fluidized bed resulted in around 10 °C, as checked by a second movable thermocouple, this value being used to correct the controller T setpoint. The reactor was housed within a 2.0 kW electric ceramic furnace (Watlow, USA) equipped with electronic temperature control (RSpro PID 1241071). The flow rates of air, N_2 , and CO_2 were regulated using three electronic flowmeters (model 5850S, Brooks, Hatfield, PA, USA), while a system of valves and a manifold enabled rapid switching of the gas stream. Gas samples were collected using a 6 mm AISI-316 probe fitted with a cellulose filter.

Silica sand with a particle size of 200–400 μm was used as the bed material, with an inventory of 60 g. In a comparative test, dolomite with same particle size was used as bed material. The minimum fluidization velocity U_{mf} of the material was 0.023 at 850 °C computed by Ergun equation (Kunii and Levenspiel, 1991), whilst the fluidization velocity U was 0.22 m/s, corresponding to a fluidization ratio $U/U_{mf} = 10$.

Every single run included a fuel pellet with a mass of 0.50 ± 0.02 g. For CO_2 gasification, the experiments have been performed at least in

triplicate, by alternating CO_2 and O_2 atmosphere, the latter step being required to avoid excessive char accumulation. During O_2 gasification, continuous feeding was performed by periodically adding a fuel pellet according to the chosen equivalence ratio. The experimental procedure comprised the following steps: (1) heating the reactor to the desired temperature in air flow, (2) switching the feed to a gas mixture for gasification at pre-set gas composition, (3) dropping a fuel pellet from the top side of the fluidization column, (4) keeping the gasification mixture for a pre-set time (t_{gas}), (5) switching the feed to air. The equivalence ratio was set between 0.30 and 0.50, corresponding to the lower range for autothermal gasification; consequently, the O_2 partial pressure in the feeding was set at $Y_{O_2} = 0.50$ to limit frequency of pellet addition. CO_2 gasification was conducted at molar fraction in the feeding $Y_{CO_2} = 0.10, 0.20$ and 0.30 , similarly to previous studies of biomass char gasification (Miccio et al., 2024).

A continuous gas analyzer (GEIT GAS 3100, Bunsbeek, Belgium) was used to determine the syngas composition. The analyzer was equipped with infrared sensors for CO , CO_2 , and CH_4 , a thermal conductivity sensor for H_2 , and an electrochemical cell for O_2 .

The gravimetric measurement of tar was performed in dedicated tests using a fixed batch of biomass, following a procedure similar to that described by Bendoni et al. (Bendon et al., 2019). During gasification, all gas exiting the reactor was directed into a glass tube filled with ceramic wool and maintained in an ice bath to facilitate tar condensation. The collected tar filters were subsequently placed in a vacuum desiccator at room temperature until a constant weight was achieved.

The tar composition was analyzed offline using a gas chromatograph (GC) (Agilent 7890A, equipped with an MSD 5975A detector, Agilent, Santa Clara, CA, USA) after extraction of the collected tar in acetone.

2.4. Data elaboration

The fuel conversion degree ξ in TG tests was computed on dry basis ($m_{0,d}$) as the ratio between the current and total combustible matter.

$$\xi = \frac{m - m_a}{m_{0,d} - m_a} \quad (1)$$

Table 1

Proximate, elemental and ash analyses of CM and BW (a.r. – as received, d.b. – dry basis, n.a. – not analyzed).

	CM	BW
Low heating value, MJ/kg (d.b.)	15.3	17.9
Proximate analysis		
Fixed C, %	17.6	13.0
Volatiles, %	59.5	73.2
Ash, %	17.7	0.8
Moisture, %	5.2	13.0
Ultimate analysis (d.b.)		
C, %	40.9	48.7
H, %	4.5	5.2
S, %	<0.1	<0.1
N, %	1.6	0.5
Cl, %	0.5	<0.1
O, % (by difference)	33.7	44.5
Ash properties		
Initial deformation temperature, °C	1180	1335
Hemispherical temperature, °C	1360	1455
Major ash components after incineration, % by mass		
SiO ₂	62.7	15.0
Al ₂ O ₃	3.3	2.5
CaO	6.2	26.0
Fe ₂ O ₃	2.3	0.5
K ₂ O	10.9	7.2
Na ₂ O	0.7	3.3
MgO	1.5	4.1
P ₂ O ₅	3.3	–
Major ash components after gasification, % by mass		
SiO ₂	61.5	n.a.
Al ₂ O ₃	5.6	
CaO	7.0	
Fe ₂ O ₃	4.6	
K ₂ O	14.4	
Na ₂ O	0.9	
MgO	1.3	
P ₂ O ₅	4.6	
Pellets properties		
Diameter, mm	10	10
Height, mm	5	6
Particle density, kg/m ³	1341	1078
Energy density, GJ/m ³	20.9	19.3
Compression strength, MPa	57.1 ± 6.0	± 4.7

The same formula applies to the char conversion degree ξ_{ch} :

$$\xi_{ch} = \frac{m - m_a}{m_{ch,d} - m_a} \quad (2)$$

The time derivative $\xi' = d\xi/dt$ was numerically calculated as the incremental ratio $d\xi/dt = \Delta\xi/\Delta t$. The activation energy E for char oxidation was obtained from the maxima of ξ' at different temperatures by linear interpolation of $\ln(\xi')$ versus $1/T$, being the slope $S = -E/RT$.

In gasification tests the yield Ψ of generic species i was computed by integration of the molar fraction profile during the gasification step, assuming the conservation of N_2 (Eq. (3)). The gas yields were determined as the total amount in mmol produced during the gasification test per gram of fed fuel. The total gas yield was computed as the sum of the yields of each component $\Psi = \sum \Psi_i$.

$$\Psi_i = \frac{1000}{m_{fuel}} \frac{Q_0}{RT} \int \frac{Y_i}{(1 - Y_{N_2})} dt \quad (3)$$

The percent carbon conversion C_{conv} was calculated (Eq. (4)) as the ratio of total carbon in gas, i.e. the sum of CO_2 , CO and CH_4 , to the total carbon in fuel, X_C being the carbon content of the fuel. In the case of CO_2 gasification, C_{conv} refers to both gasification and oxidation stages.

$$C_{conv} = \frac{\Psi_{CO_2} + \Psi_{CO} + \Psi_{CH_4}}{X_C} 0.012\% \quad (4)$$

The cold gas efficiency CGE (Eq. (5)) was calculated taking into account the low heating value LHV_{gas} of produced syngas per standard cubic meter and LHV_{fuel} per kilogram of fuel.

$$CGE = \Psi RT \frac{1}{1000} \frac{LHV_{gas}}{LHV_{fuel}} \quad (5)$$

The tar yield φ was computed as the ratio between the collected tar and the fuel mass:

$$\varphi = m_{tar}/m_{fuel} \quad (6)$$

3. Results and discussion

3.1. TG results

Fig. 3-a displays the comparison between the weight decrease profiles obtained in the N_2/CO_2 atmosphere at 850 °C for BW and CM, upon

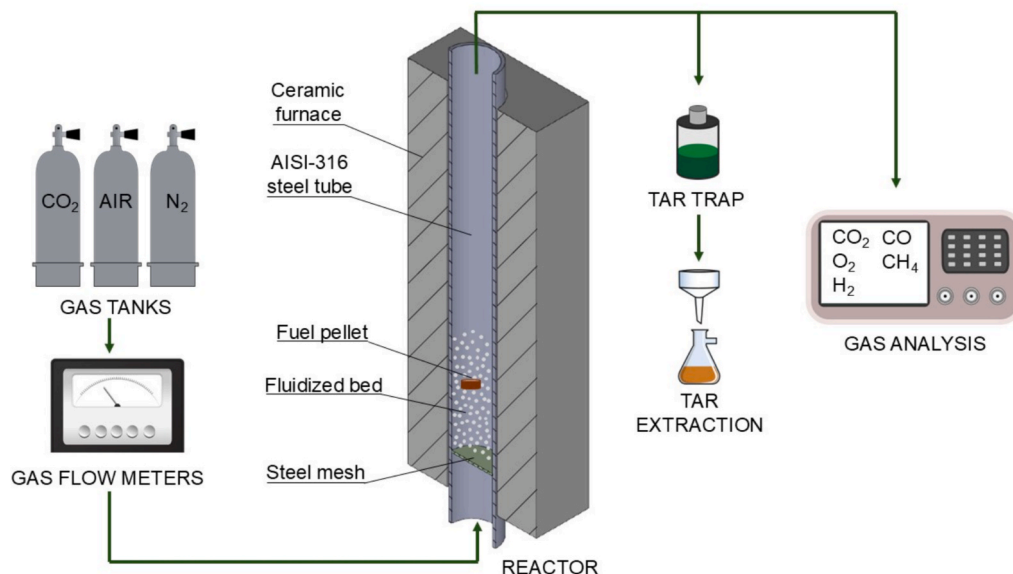


Fig. 2. Laboratory scale plant for gasification.

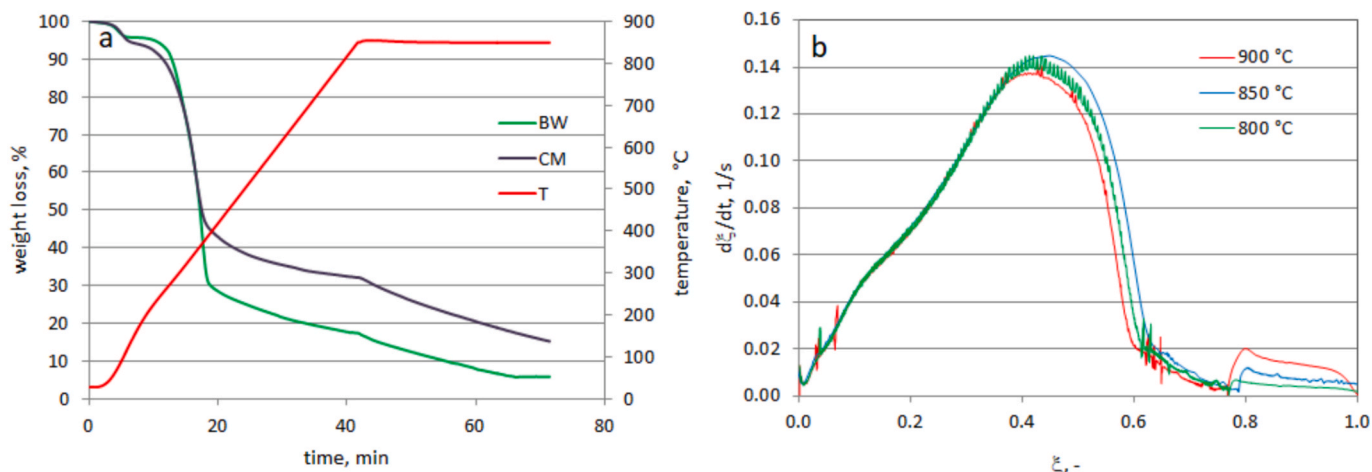


Fig. 3. TG results at heating rate of 20 K/min in N_2 up to 850 °C and isothermal segment (30 min) at 850 °C in N_2/CO_2 ; a) weight loss for BW and CM, b) dimensionless conversion rate of CM versus conversion degree.

initial heating in inert conditions. Stages of drying (up to 100 °C) and devolatilization are well evident for both fuels during heating in N_2 . The devolatilization appears to last longer for CM, up to $t = 25$ min corresponding to 500 °C, than for BW. As the temperature reached 850 °C and the atmosphere was changed to N_2/CO_2 , the weight slowly decreased, achieving the ash final value.

It also appears that the last segment (i.e. char oxidation from time 40 min) is shorter for BW with respect to CM, as consequence of the higher fixed carbon content in CM (17.6 %) with respect to BW (13.0 %). In fact, the larger ash content of CM could reduce the interparticle diffusion but can also catalytically enhance the oxidation kinetics due to the presence of elements, such as Ca and K (Xue et al., 2024). It is worth noting that, according to proximate and ultimate analysis of the fuels (Table 1), the char accounts for around 50 % of the total heating value.

The dimensionless conversion rate $d\xi/dt$ of CM is displayed in Fig. 3-b at different temperatures and in N_2/CO_2 atmosphere. The profiles are overlapping during the devolatilization ($\xi < 0.75$), whilst they are well distinct during char oxidation on the right end of the diagram. Congruently, the kinetics increases with the temperature, showing a peak at the beginning of the char oxidation when intra-particle diffusion resistance is less relevant. The maxima of ξ' referred to CM char oxidation (Eq. (2)) were calculated for both N_2/CO_2 and O_2 atmosphere, obtaining values of order of magnitude equal to 10^{-4} and 10^{-3} , respectively. This large difference is reflected in the computed activation energy E that is equal to 87 kJ/mol for O_2 , and 122 kJ/mol for CO_2 . Such values are consistent with those reported for woody biomass (Wu et al.,

2023) and depend greatly on the oxidizing agent, CO_2 being less reactive (Laurendeau, 1978). For comparison, the literature reports only a few data on CM with *iso-conversional* methods under pyrolysis conditions: Akyurek calculated the activation energy of CM using the Flynn–Wall–Ozawa method as 195 kJ/mol (Akyurek, 2019) while Yuan et al. as 119–348 kJ/mol, depending on the conversion rate (Yuan et al., 2017).

3.2. Gasification results: Gas composition, yields and cold gas efficiency

Volumetric fractions (Y) of CO , CO_2 , O_2 , CH_4 , and H_2 during the gasification of CM in CO_2 atmosphere at $Y_{CO_2} = 0.20$ are presented in Fig. 4a. Similarly, Fig. 4b displays Y_{CO} , Y_{CO_2} , Y_{O_2} , Y_{CH_4} , and Y_{H_2} during CM gasification in O_2 atmosphere at $\chi = 0.3$, every peak in the graphs representing one single fuel pellet fed into the reactor.

In the case of O_2 gasification, the fuel feeding had a variable period to maintain the desired equivalence ratio, i.e. 55, 70 and 90 s for CM. Moreover, in both cases a semi-continuous and periodic process was carried out, appearing well repeatable after a few steps. For O_2 gasification, Y_{O_2} achieved null value after only three cycles. The bed and remaining ashes were removed from the reactor to ensure reliable operation after a certain number of tests. In some cases, pellets containing ash and traces of carbon were recovered, rather similar in shape to the original ones although shrinkage was evident (see section 3.4). The tests carried out with BW resulted in higher peaks of all measured species as consequence of the observed faster devolatilization kinetics in

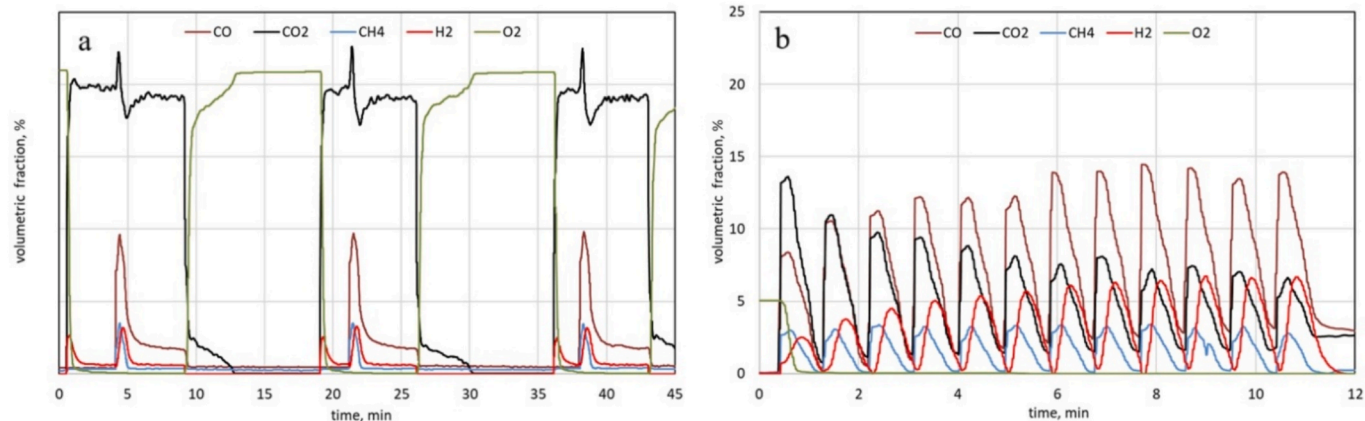


Fig. 4. Volumetric fractions of CO , CO_2 , CH_4 , H_2 and O_2 a) for CO_2 gasification of CM at $Y_{CO_2} = 0.20$; b) for O_2 gasification of CM at $\chi = 0.3$ (silica sand bed).

TGA tests. In CO₂ atmosphere, the occurrence of carbon gasification led to lower Y_{CO2} after the devolatilization of the pellet (Fig. 4a). On the contrary, in the case of O₂ gasification, the CO₂ time profile follows that of CO (Fig. 4b), as the two species are in chemical equilibrium in the presence of carbon. A decrease of the CO₂ peak per single pellet can be noted as a consequence of carbon accumulation in the bed.

Table 2 reports the overall results of the tests conducted for both fuels, including the yields of combustible syngas components (CO, CH₄, and H₂), carbon conversion (C_{conv}), maximum lower heating value of syngas (LHV_{max}), cold gas efficiency (CGE), tar yields φ, and molar shares of (AU < 200) and heavy (AU > 200) tar components. For CM, three levels of equivalence ratio, i.e. χ = 0.30, 0.40 and 0.50, have been selected corresponding to increasing auto-thermal conditions, higher than the ideal optimum value χ = 0.26, to enhance carbon and tar conversion in the lab scale FB plant (Sikarwar et al., 2016).

The closure of carbon balance was checked on the basis of C_{conv} data. For O₂ gasification, the carbon conversion was already over 85.0 %, with the largest value 98.2 % for BW, the balance to 100 being the accumulation of the char in the bed that was undetected. For CO₂ gasification, the total carbon conversion, sum of gasification and oxidation steps, was always close to 100 %, since in the O₂ step the accumulated char was burnt.

The yields of CO, CH₄, and H₂ for CM gasification are presented in Fig. 5a for O₂ gasification and in 5b for CO₂ gasification, respectively.

In the case of CO₂ gasification, the highest volumetric fractions of CO (10.4 %), H₂ (3.6 %), and CH₄ (3.4 %) were achieved at Y_{CO2} = 0.30 resulting in the maximum LHV of syngas 2.92 MJ/m³. For comparison, at Y_{CO2} = 0.10 the highest volumetric fractions for BW were 16.4 % CO, 4.9 % CH₄, and 8.5 % H₂, with maximum LHV of syngas 4.74 MJ/m³.

In case of O₂ gasification, the highest volumetric fractions of 14.4 % CO, 3.4 % CH₄, and 7.7 % H₂ were achieved at χ = 0.3, resulting in the maximum LHV of syngas 4.37 MJ/m³. For comparison, at χ = 0.3 and χ = 0.5 for BW the maximum LHV of syngas was 6.06 and 4.20 MJ/m³, respectively (Tab.2). The higher volatiles content of BW (Tab. 1) being the main reason of the larger yield in CH₄ and H₂ with respect to CM, contributing to produce a more energetic syngas.

The observed trends are consistent with the variation of the equivalence ratio and the CO₂ feeding molar fraction. In O₂ gasification, increasing χ led to decreasing yields of CO, CH₄ and H₂, while the overall carbon conversion slightly increased. This is reflected in the decline of LHV and CGE, as higher ER promotes further oxidation of combustible species and increased CO₂ formation. In contrast, during CO₂ gasification all performance indicators improved with increasing Y_{CO2} from 0.0 to 0.30. In particular, the CO yield increased markedly (up to 31 mmol/g

compared with 18 mmol/g in O₂ gasification) due to the inverse Boudouard reaction, while CH₄ yield remained nearly constant, being mainly related to volatile conversion. H₂ yield changed only marginally, as its main generation pathway was dry reforming of volatiles in the presence of excess CO₂ (Hanf et al., 2022). Conversely, during O₂ gasification the larger the equivalence ratio, the higher the shift toward full hydrogen oxidation (Basu, 2010).

Since catalytic gasification of biomass is extensively covered by the literature (Abu El-Rub et al., 2004), only a comparative and exploratory test was done using silica sand (inert) and dolomite (catalytic) as bed materials during CM gasification only in O₂ atmosphere at χ=0.35. CO and CH₄ yields were comparable in both inert and catalytic beds and similar to value reported in Table 2. Conversely, H₂ yield increased, reaching a value of 13.0 ± 0.5 mmol/g well higher than corresponding data in Table 2 at χ=.30 and 0.40. The presence of dolomite primarily contributed to the reduction of tar species (Miccio et al., 2016), leading to increase H₂ and CH₄ generation, with the latter being partially offset by concurrent steam and dry reforming reactions that are favored by the catalyst. The obtained H₂ yield aligns well with reported literature values for biomass gasification (Song et al., 2022).

3.3. Gasification results: Tar behavior

In addition to gaseous products, tar formation is a critical parameter in evaluating the quality of the syngas produced during biomass gasification. Some experimental tests were purposely conducted to determine the tar yield for CM and BW under the same operating conditions in inert bed. Table 2 reports the obtained results in terms of specific tar yield φ and share between light and heavy components. In every case, the values of φ were lower than 10 mg/g for both fuels, being well acceptable in a fluidized bed gasifier in the absence of a catalyst (Miccio et al., 2016). The tar yield was higher in the case of CM, the difference being more pronounced for O₂ gasification. The CO₂ gasification resulted in higher tar yield with respect to oxygen gasification but for CM the increase in φ was lower than for BW, i.e. 1.1 versus 1.8 times, indicating that the rather low value φ = 3.77 mg/g for BW in the air was probably due to the tar oxidation in freeboard that occurs more likely in presence of O₂ and H₂O produced by oxidation of volatiles. Conversely, carbon dioxide is less effective in tar cracking and reforming due to the absence of H radicals that are indispensable for the cracking of aromatics (Tang et al., 2023).

The share between light (AU < 200) and heavy (AU > 200) tar components was determined by the GC analysis of tar extracted in acetone and showed the prevalence of typical aromatic compounds with

Table 2
Gas yields, carbon conversion, CGE and tar yields during gasification in CO₂ and O₂ (silica sand bed).

Fuel	Equivalence ratio — CO ₂ fraction	CO yield mmol/g	CH ₄ yield mmol/g	H ₂ yield mmol/g	C _{conv} gasification %	C _{conv} oxidation %	LHV _{max} MJ/Nm ³	CGE %
O ₂ gasification								
CM	χ=0.3	18.4 ± 0.8	3.5 ± 0.1	4.9 ± 0.6	85.6 ± 2.3	—	4.37	60.0
CM	χ =0.4	15.4 ± 0.5	3.9 ± 0.1	4.9 ± 0.7	86.0 ± 2.2	—	3.33	57.1
CM	χ =0.5	11.7 ± 0.4	3.8 ± 0.1	5.1 ± 0.7	88.3 ± 2.2	—	2.62	40.0
BW	χ =0.3	18.3 ± 1.0	4.2 ± 0.4	12.5 ± 0.8	93.7 ± 2.0	—	6.06	84.0
BW	χ =0.5	15.0 ± 2.0	5.9 ± 0.2	6.7 ± 0.2	98.2 ± 2.0	—	4.20	58.3
CO ₂ gasification								
CM	N ₂	8.9 ± 0.2	3.2 ± 0.1	1.6 ± 0.4	63.4 ± 1.6	36.9 ± 0.9	2.48	40.4
CM	Y _{CO2} = 0.10	22.9 ± 0.6	3.8 ± 0.2	1.5 ± 0.1	70.8 ± 1.7	31.6 ± 0.8	2.57	64.6
CM	Y _{CO2} = 0.20	26.5 ± 0.5	4.3 ± 0.8	1.4 ± 0.1	73.5 ± 1.8	28.0 ± 0.7	2.69	73.9
CM	Y _{CO2} = 0.30	31.2 ± 1.2	4.2 ± 0.2	2.0 ± 0.4	73.7 ± 1.8	30.7 ± 0.7	2.92	83.1
BW	Y _{CO2} = 0.10	36.8 ± 1.9	5.3 ± 0.3	6.0 ± 1.0	88.3 ± 2.2	11.0 ± 0.4	4.74	90.1
Tar yields								
Fuel	Atmosphere	Tar yield φ, mg/g		Share of light (AU < 200) tar components			Share of heavy (AU > 200) tar components	
CM	CO ₂ - Y _{CO2} = 0.20	8.4 ± 0.1		0.58			0.42	
BW	CO ₂ - Y _{CO2} = 0.20	6.7 ± 0.1		0.77			0.23	
CM	O ₂ - χ = 0.40	7.4 ± 0.1		0.60			0.49	
BW	O ₂ - χ = 0.40	3.7 ± 0.1		0.71			0.29	

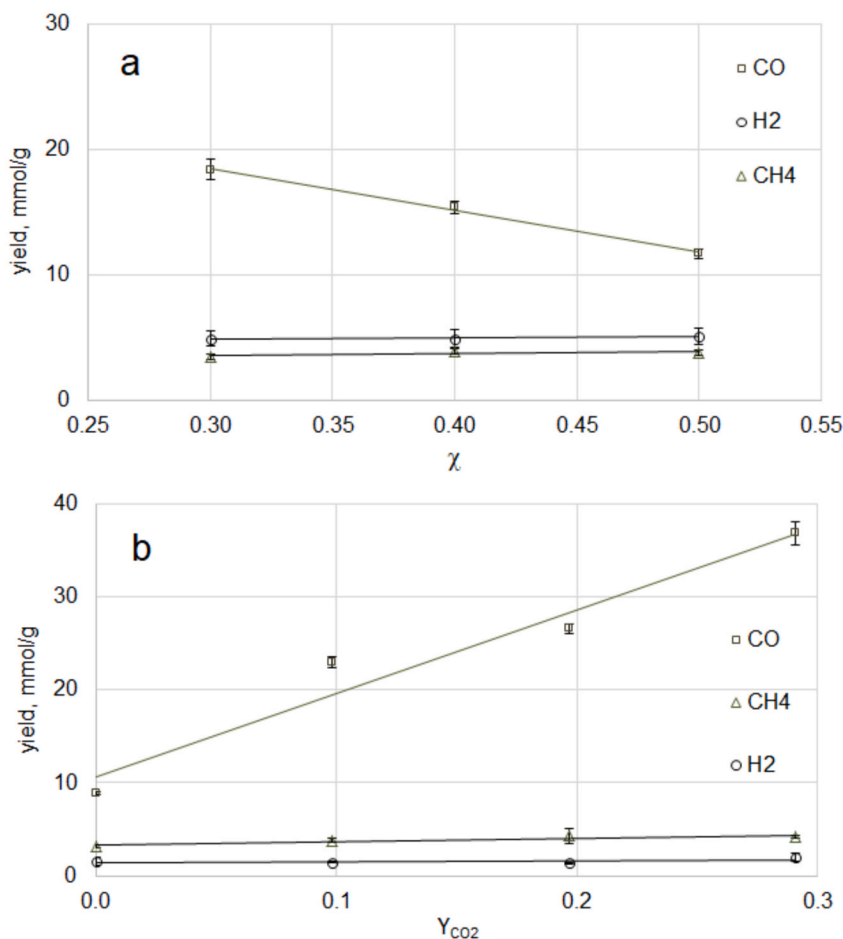


Fig. 5. Gas yields upon gasification of CM in a) O₂ and b) CO₂ (silica sand bed).

3–5 rings, e.g. anthracene, pyrene, and benzo-pyrene. The presence of amides (dodecanamide, tetradecanamide, octadecanamide) was also revealed in CM tar, as consequence of the rather high nitrogen content in the biomass. There is little difference between CM and BW although a higher content, around 30 %, of heavy tar can be appreciated for CM. The gasification atmosphere did not substantially change the ratio between the two tar classes, unlike what was observed for the yield.

Overall, the comparative study on tar yield and characteristics proved that both fuels had similar behavior. Consequently, already investigated methods for tar conversion and abatement, e.g. in-situ or downstream catalysis, scrubbing, and adsorption (Cortazar et al., 2023), are expected to be effective also for CM gasification.

3.4. Gasification results: Ash behavior

As consequence of the large ash content (17.7 %wt), the ash behavior is a relevant issue during CM conversion. As reported in Table 1, the characteristic ash fusion temperatures are lower for CM with respect to BW, with a difference of around 150 °C for initial deformation and 100 °C for hemispherical temperature. This can be ascribed to the higher content of Si together with the presence of K and Cl in CM. Therefore, the appearance of low-melting chlorine and alkali compounds and eutectics in the ash is possible (Miles et al., 1996). Nevertheless, the measured values, all above 1000 °C, indicate that under the operating temperature applied in this study (850 °C) the ash remains stable, the temperature of the char particles during gasification being not much higher than that of the fluidized bed (Scala, 2011). This explains why no bed agglomeration or defluidization was observed, confirming that the relatively high ash

fusion temperatures of investigated CM are a distinctive and favorable feature of this specific fuel type (Maj, 2022; Maj et al., 2022, Maj et al., 2021). These properties significantly reduce the likelihood of bed agglomeration under the operating conditions applied in the presented experiments.

The gasification of CM proved that the residual ash exhibits the original shape of the pellet, as shown in Fig. 1, displaying a char pellet obtained during gasification (e) and completely converted ash pellets (f). The char pellet retains around 30 % of original weight and possesses still sufficient hardness, whilst the ash pellets are friable and likely undergo comminution, this latter being favored at higher fluidization velocity. Solid CM residues recovered from gasification tests have been characterized by ICP analysis and results reported in Table 1, showing a prevalence of Si, K, Ca and Al oxides. The XRD pattern of CM ashes is shown in Fig. 6. The spectrum reveals a dominant quartz signal indicated by the star symbols in the figure, which significantly overshadows other phases, making it challenging to precisely quantify both crystalline components and the amorphous fraction. Nevertheless, the presence of another SiO₂ polymorph suggests that a portion of the silica may indeed be amorphous. The remaining identified phases mainly consist of potassium chloride and various aluminosilicates, which align well with the oxide composition reported in Table 1. Chlorine, mostly present in biomass as salt-bound forms (e.g., potassium chloride KCl), may either volatilize or remain in the solid residue depending on process conditions and interactions with other ash components. The XRD analysis of ash revealed the presence of KCl in the residual solid, indicating that part of the chlorine is retained in the ash phase. The inset in Fig. 6 shows the SEM image of the samples, confirming the presence of an amorphous

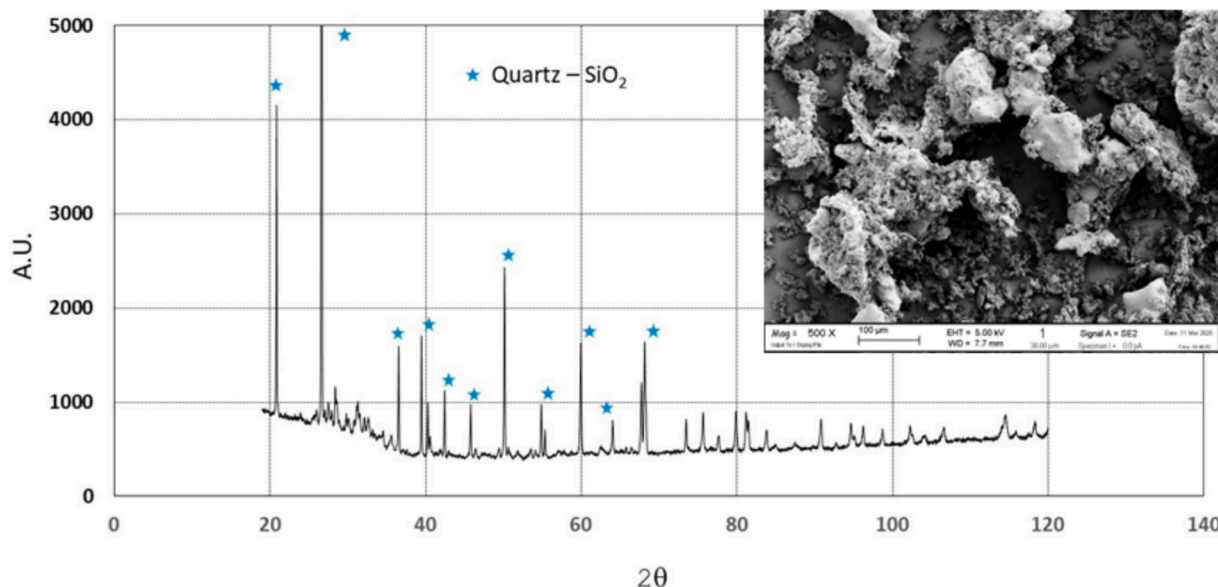


Fig. 6. XRD pattern and SEM image (inset) of the CM ash after gasification.

phase, with few relevant ordered structures in form of small crystallizations, as well as some spherules.

4. Discussion

To better understand the significance of the obtained results, the discussion in light of existing knowledge, current biomass market and potential applications is required. While various biomass sources such as wood, agricultural residues, and dedicated crops are commonly used in gasification, CM is an underutilized feedstock although it is widely available (Font-Palma, 2019; Maj et al., 2024). Unlike agricultural byproducts or crop residues, which might be in competition with animal feed or raw materials, manure's disposal methods are typically limited to land spreading or composting. Using it in thermal processes could represent a more sustainable option, reducing disposal costs, release of odors, and uncontrolled methane emissions, being the consequence of the open-air decomposition (Baldé et al., 2016). What is more, the utilization of carbon dioxide as a gasifying agent offers significant environmental advantages in the context of CO₂ management and greenhouse gas mitigation. Piggery waste and horse manure were also investigated in terms of thermal conversion (Zhao et al., 2025). Nevertheless, in piggery farming, a bedding-free environment is frequently implemented, using the technology of slatted floors (Devilleers et al., 2020). The waste obtained in this way is semi-liquid, and therefore its suitability for thermal conversion is low.

The marked heterogeneity and shapelessness of CM was appropriately addressed by pelleting, which allowed the homogenization of the material and the obtaining of regular granules, reducing the variability of the properties and ensuring more reliable process. It is worth noting that pelleting was done without additives, since during compression lignin and proteins, naturally present in the manure, acted as binders. The process may be further enhanced by increasing the temperature, favoring lignin penetration into adjacent particles and strengthening the whole pellet (Ma et al., 2021).

Gasifiers typically designed for higher-energy and lower-moisture feedstocks may require modifications to handle manure effectively. However, advanced gasification technology, such as fluidized beds, is promising in processing challenging feedstocks, including manure (Akbarian et al., 2022). It cannot be ignored that while biomass may be seasonal or location-dependent, CM is consistently available throughout the year and well distributed. Already existing large-scale gasification plants can be co-fed by CM unless the transportation does not

significantly impact the economics and environmental sustainability. On the contrary, small-scale gasification plants (less than 1.0 MWh), even transportable, could prove very interesting for operation close to cattle farms, valorizing the energy content of the residual biomass, in a circular economy perspective (Turzyński et al., 2022) and contemporary reducing the large emissions of CO₂ and contaminants in the atmosphere deriving from the uncontrolled CM disposal.

The CM can be thermally converted with other animal waste. The copyrolysis of CM and PL showed a synergistic improvement in the reaction kinetics and the production of combustible syngas components, such as H₂ and CO (Goud Burra et al., 2023), likely due to the catalytic effect of char formed early from chicken manure decomposition, which takes place at lower temperature levels (Selim and Amano, 2021). This supports the potential for developing a technology for manure conversion capable of handling mixed manure feedstocks, which could benefit various animal farming operations. When it comes to economic feasibility, animal waste is characterized by a significantly lower price than conventional biomass. CM is not listed on traditional biofuel markets, so when determining its price, one can only rely on the average price per ton based on agricultural price quotations, which in Poland is approximately 14 EUR/t. Assuming its LHV of 15 MJ/kg, a cost of 3.4 EUR/MWh can be calculated. For comparison, according to the international Belpool biomass market, the cost of energy from wood chips reaches 30 EUR/MWh.

Concerning the two investigated options, i.e. O₂ and CO₂ gasification, the following aspects should be considered: The gasification in the air can be easily carried out under autothermal conditions for an equivalence factor greater than 0.3 (Miccio et al., 2024) but the produced syngas is diluted by air N₂. On the contrary, the gasification in CO₂ is always allo-thermal because the fundamental reaction of carbon gasification by CO₂ has a standard enthalpy equal to 172.4 kJ/mol and the process requires external heat supply (Pinto et al., 2016). For what concerns the tar yield, the research proved that air gasification is better than CO₂ gasification, minimizing the need of measures for tar abatement before syngas utilization (Abu El-Rub et al., 2004). Overall, regarding a scenario of small-scale implementation and poor economy, although CO₂ gasification is appealing from the environmental sustainability perspective, it is believed that we should move towards air gasification with immediate use of the syngas. The CO₂ option would reasonably require higher CAPEX and can be considered for large-scale implementation.

Since CM char pellets are enough hard-wearing, their recovery

before complete conversion would represent a possible advantage for the process, avoiding excessive load in cyclone and filters downstream the gasifier caused by the entrained ash fines. Such char granules can be conveniently used as fertilizer and soil improver in agriculture (Osman et al., 2022) or used as an additive in composting of organic waste (Wang and Akdeniz, 2023). Manure-derived biochar are also characterized by excellent sorption performance (Wang et al., 2024). Conversely, in the case of complete thermal conversion, a possible exploitation of CM ash would be the production of geopolymer artifacts (Miccio et al., 2014), owing to the presence of Si, Al and Ca oxides in the ash composition and amorphous phase (Fig. 6). In fact, the composition of ashes indicates potential for geopolymerization, as the aluminosilicates, particularly muscovite, which is also found in highly reactive precursors like metakaolin, and the amorphous silica fraction can be considered active phases in alkali activation. A more detailed quantification of the amorphous aluminosilicate phases would be useful to better define the material's $\text{SiO}_2/\text{Al}_2\text{O}_3$ ratio, thus enabling the selection of the most suitable activator system (alkali silicate and/or hydroxide). In any case, the phases identified as non-reactive, such as quartz and sylvite, do not negatively impact the formation of the binding phase: quartz can act as a stabilizing filler, while sylvite can be easily removed from the consolidated system through post-treatment washing to prevent efflorescence formation.

5. Conclusions

This study investigated the fluidized bed gasification of pelletized CM under CO_2 and O_2 atmospheres at 850 °C. The main findings are:

- (1) Pelletization of CM proved to be an effective pretreatment, producing stable and homogeneous pellets with higher energy density than wood, facilitating reliable feeding and handling.
- (2) The thermo-gravimetric investigation determined the activation energy of the CM char oxidation, under O_2 and CO_2 atmosphere, providing for the first time suitable parameters, i.e. 87 and 122 kJ/mol respectively, to be used in mathematical kinetic models.
- (3) Gasification performance showed that for the CO_2 gasification, an increase in CO_2 fraction favors the conversion of CM to syngas. Gas yields of H_2 , CH_4 , and CO were the highest at $Y_{\text{CO}_2} = 0.30$ with a conversion of 73.7 %. For the O_2 atmosphere, the decrease in equivalence ratio resulted in higher yields of syngas components. At $\chi = 0.3$ fuel conversion of 86.4 % and cold gas efficiency of 60 % were achieved, whilst the highest hydrogen yield was 6.10 mmol in catalytic (dolomite) bed.
- (4) Tar formation was low (<10 mg/g) in all cases, comparable between CM and BW, with slightly higher yields for CM and a larger share of heavy components.
- (5) Ash behavior of CM was favorable: despite slightly lower fusion temperatures than BW, CM ashe exhibited melting point > 1000 °C, therefore avoiding agglomeration under the tested conditions. The ash composition, rich in Si and Al oxides with an amorphous fraction, suggests potential for utilization in geopolymer applications.

These results demonstrate that cattle manure can be efficiently gasified in fluidized bed reactors, producing syngas with satisfactory quality, low tar content, and stable operation without bed agglomeration.

CRedit authorship contribution statement

Francesco Miccio: Writing – original draft, Supervision, Methodology, Investigation, Funding acquisition. **Izabella Maj:** Writing – original draft, Visualization, Methodology, Investigation, Supervision, Funding acquisition. **Lucrezia Polchri:** Visualization, Investigation. **Annalisa Natali Murri:** Investigation, Data curation.

Declaration of competing interest

The authors declare that they have no known competing financial interests or personal relationships that could have appeared to influence the work reported in this paper.

Acknowledgments

This research was supported by National Science Centre, Poland, grant number 2021/43/D/ST8/02609 “The influence of aluminosilicate additives on high-temperature corrosion and ash properties of animal-origin biomass”.

The research has been funded by the Italian National Programme “Ricerca e Sviluppo di Tecnologie per la Filiera dell’Idrogeno - ADP Italian Ministry MiTE - ENEA, Mission 2, Comp. 2.3.5, PNRR, 2022-2025, L.A. 1.1.23”.

Data availability

The data is available at <https://doi.org/10.18150/T4WBWG>.

References

- Abu El-Rub, Z., Bramer, E.A., Brem, G., 2004. Review of Catalysts for Tar Elimination in Biomass Gasification Processes. *Ind. Eng. Chem. Res.* 43, 6911–6919. <https://doi.org/10.1021/ie0498403>.
- Akbarian, A., Andooz, A., Kowsari, E., Ramakrishna, S., Asgari, S., Cheshmeh, Z.A., 2022. Challenges and opportunities of lignocellulosic biomass gasification in the path of circular bioeconomy. *Bioresour. Technol.* 362, 127774. <https://doi.org/10.1016/j.biortech.2022.127774>.
- Akter, Mst.M., Surovy, I.Z., Sultana, N., Faruk, Md.O., Gilroyed, B.H., Tijing, L., Arman, Didar-ul-Alam, Md., Shon, H.K., Nam, S.Y., Kabir, M.M., 2024. Techno-economics and environmental sustainability of agricultural biomass-based energy potential. *Appl. Energy* 359, 122662. DOI: 10.1016/j.apenergy.2024.122662.
- Akyürek, Z., 2019. Sustainable Valorization of Animal Manure and Recycled Polyester: Co-pyrolysis Synergy. *Sustainability* 11, 2280. <https://doi.org/10.3390/su11082280>.
- Al Zahra, W., Ikhsan Shiddieqy, M., Anisa, R., Yani, A., Priyo Purwanto, B., 2024. The dynamics of nitrous oxide and methane emissions from various types of dairy manure at smallholder dairy farms as affected by storage periods. *Waste Manag.* 183, 10–20. <https://doi.org/10.1016/j.wasman.2024.04.039>.
- Al-Rumaihi, A., Shahbaz, M., Mckay, G., Al-Ansari, T., 2023. Investigation of co-pyrolysis blends of camel manure, date pits and plastic waste into value added products using Aspen Plus. *Fuel* 340, 127474. <https://doi.org/10.1016/j.fuel.2023.127474>.
- Ashraf, M., Ramzan, N., Azam, M., Anwar, A., Khan, R.U., Durrani, A.K., Rashid, M.U., 2022. Cattle dung conversion to syngas: solar photovoltaic integrated gasification system. *Biomass Convers. Biorefin.* <https://doi.org/10.1007/s13399-022-02978-0>.
- Baldé, H., VanderZaag, A.C., Burtt, S.D., Wagner-Riddle, C., Crolla, A., Desjardins, R.L., MacDonald, D.J., 2016. Methane emissions from digestate at an agricultural biogas plant. *Bioresour. Technol.* 216, 914–922. <https://doi.org/10.1016/j.biortech.2016.06.031>.
- Basu, P., 2010. Chapter 5 - Gasification Theory and Modeling of Gasifiers. In: *Biomass Gasification and Pyrolysis. Practical Design*. Academic Press, pp. 117–165.
- Bendoni, R., Miccio, F., Medri, V., Benito, P., Vaccari, A., Landi, E., 2019. Geopolymer composites for the catalytic cleaning of tar in biomass-derived gas. *Renew. Energy* 131, 1107–1116. <https://doi.org/10.1016/j.renene.2018.08.067>.
- Burra, K.G., Hussein, M.S., Amano, R.S., Gupta, A.K., 2016. Syngas evolutionary behavior during chicken manure pyrolysis and air gasification. *Appl. Energy* 181, 408–415. <https://doi.org/10.1016/j.apenergy.2016.08.095>.
- Cai, W., Luo, Z., Zhou, J., Wang, Q., 2021. A review on the selection of raw materials and reactors for biomass fast pyrolysis in China. *Fuel Process. Technol.* 221, 106919. <https://doi.org/10.1016/j.fuproc.2021.106919>.
- Chen, Z., Jiang, X., 2014. Microbiological Safety of Chicken Litter or Chicken Litter-based Organic Fertilizers: a Review. *Agriculture* 4, 1–29. <https://doi.org/10.3390/agriculture4010001>.
- Constantinescu, M., Bucura, F., Ionete, E.I., Spiridon, Ş.-I., Ionete, R.E., Zaharioiu, A., Marin, F., Ion-Ebrasu, D., Botoran, O.R., Roman, A., 2024. Cattle manure thermochemical conversion to hydrogen-rich syngas, through pyrolysis and gasification. *Int. J. Hydrogen Energy* 79, 1058–1070. <https://doi.org/10.1016/j.ijhydene.2024.07.102>.
- Cortazar, M., Santamaria, L., Lopez, G., Alvarez, J., Zhang, L., Wang, R., Bi, X., Olazar, M., 2023. A comprehensive review of primary strategies for tar removal in biomass gasification. *Energy Convers Manag* 276, 116496. <https://doi.org/10.1016/j.enconman.2022.116496>.
- Devillers, N., Yan, X., Dick, K.J., Zhang, Q., Connor, L., 2020. Determining an effective slot and gap width of flooring for group sow housing, considering both sow comfort and ease of manure management. *Livest. Sci.* 242, 104275. <https://doi.org/10.1016/j.livsci.2020.104275>.

- Ersoy, A.E., Ugurlu, A., 2024. Bioenergy's role in achieving a low-carbon electricity future: a case of Türkiye. *Appl. Energy* 372, 123799. <https://doi.org/10.1016/j.apenergy.2024.123799>.
- Font-Palma, C., 2019. Methods for the Treatment of cattle Manure—A Review. *C (basel)* 5, 27. <https://doi.org/10.3390/c5020027>.
- Gabbielli, R., Seggiani, M., Frigo, S., Puccini, M., Vitolo, S., Raggio, G., Puccioni, F., 2016. Validation of a Small Scale Woody Biomass Downdraft Gasification Plant coupled with Gas Engine. *Chem. Eng. Trans.* 50, 241–246.
- Goud Burra, K.R., Selim, O.M., Amano, R.S., Gupta, A.K., 2023. Synergy in Syngas Yield from Co-Pyrolysis of Cow and Chicken Manures. *J. Energy Res. Technol.* 145. <https://doi.org/10.1115/1.4056563>.
- Hanf, S., Angeli, S., Dussol, D., Fritsch, C., Maier, L., Müller, M., Deutschmann, O., Schunk, S.A., 2022. Methane Dry Reforming, in: *Chemical Valorisation of Carbon Dioxide*. The Royal Society of Chemistry, pp. 187–207. DOI: 10.1039/9781839167645-00187.
- Hussein, M.S., Burra, K.G., Amano, R.S., Gupta, A.K., 2017. Temperature and gasifying media effects on chicken manure pyrolysis and gasification. *Fuel* 202, 36–45. <https://doi.org/10.1016/j.fuel.2017.04.017>.
- Kong, G., Zhang, X., Wang, K., Li, J., Zhou, L., Wang, J., Zhang, X., Han, L., 2023. Coupling biomass gasification and inline co-steam reforming: Synergistic effect on promotion of hydrogen production and tar removal. *Fuel Process. Technol.* 243, 107689. <https://doi.org/10.1016/j.fuproc.2023.107689>.
- Kunii, D., Levenspiel, O., 1991. Fluidization and Mapping of Regimes, in: *Fluidization Engineering*. Elsevier, pp. 61–94. DOI: 10.1016/B978-0-08-050664-7.50009-3.
- Kwon, G., Cho, D.-W., Hyun Moon, D., Kwon, E.E., Song, H., 2019. Beneficial use of CO₂ in pyrolysis of chicken manure to fabricate a sorptive material for CO₂. *Appl. Therm. Eng.* 154, 469–475. <https://doi.org/10.1016/j.applthermaleng.2019.03.110>.
- Laurendeau, N.M., 1978. Heterogeneous kinetics of coal char gasification and combustion. *Prog. Energy Combust. Sci.* 4, 221–270. [https://doi.org/10.1016/0360-1285\(78\)90008-4](https://doi.org/10.1016/0360-1285(78)90008-4).
- Ma, J., Feng, S., Shen, X., Zhang, Z., Wang, Z., Kong, W., Yuan, P., Shen, B., Mu, L., 2021. Integration of the pelletization and combustion of biodried products derived from municipal organic wastes: the influences of compression temperature and pressure. *Energy* 219, 119614. <https://doi.org/10.1016/j.energy.2020.119614>.
- Ma, M., Wang, J., Song, X., Su, W., Bai, Y., Yu, G., 2020. Co-Gasification of Cow Manure and Bituminous Coal: a Study on Reactivity, Synergistic effect, and Char Structure Evolution. *ACS Omega* 5, 16779–16788. <https://doi.org/10.1021/acsomega.0c01785>.
- Maj, I., 2022. Significance and challenges of Poultry Litter and cattle Manure as Sustainable Fuels: a Review. *Energies (basel)* 15, 8981. <https://doi.org/10.3390/en15238981>.
- Maj, I., Kalisz, S., Ciukaj, S., 2022. Properties of Animal-Origin Ash—A Valuable Material for Circular Economy. *Energies (basel)* 15. <https://doi.org/10.3390/en15041274>.
- Maj, I., Kalisz, S., Szymajda, A., Łaska, G., Golombek, K., 2021. The influence of cow dung and mixed straw ashes on steel corrosion. *Renew. Energy* 177. <https://doi.org/10.1016/j.renene.2021.06.019>.
- Maj, I., Niesporek, K., Matus, K., Miccio, F., Mazzocchi, M., Lój, P., 2024. The Impact of Aluminosilicate Additives upon the Chlorine distribution and Melting Behavior of Poultry Litter Ash. *Energies (basel)* 17, 1854. <https://doi.org/10.3390/en17081854>.
- Miccio, F., Medri, V., Papa, E., Natali Murri, A., Landi, E., 2014. Geopolymerization as Effective measure for reducing risks during Coal Ashes Handling, Storage and Disposal. *Chem. Eng. Trans.* 36, 133–138. <https://doi.org/10.3303/CET1436023>.
- Miccio, F., Picarelli, A., Ruoppolo, G., 2016. Increasing tar and hydrocarbons conversion by catalysis in bubbling fluidized bed gasifiers. *Fuel Process. Technol.* 141, 31–37. <https://doi.org/10.1016/j.fuproc.2015.06.007>.
- Miccio, F., Polchri, L., Murri, A.N., Landi, E., Medri, V., 2024. Chemical looping gasification of biomass char in fluidized bed and CO₂-enriched atmosphere. *Biomass Convers. Biorefin.* <https://doi.org/10.1007/s13399-024-06059-2>.
- Miles, T.R., Miles, T.R., Baxter, L.L., Bryers, R.W., Jenkins, B.M., Oden, L.L., 1996. Boiler deposits from firing biomass fuels. *Biomass Bioenergy* 10. [https://doi.org/10.1016/0961-9534\(95\)00067-4](https://doi.org/10.1016/0961-9534(95)00067-4).
- Moffo, F., Mouiche, M.M.M., Djomgang, H.K., Tombe, P., Wade, A., Kochivi, F.L., Dongmo, J.B., Mbah, C.K., Mapiéfou, N.P., Ngogang, M.P., Awah-Ndukum, J., 2021. Poultry Litter Contamination by *Escherichia coli* Resistant to Critically Important Antimicrobials for Human and Animal Use and risk for Public Health in Cameroon. *Antibiotics* 10, 402. <https://doi.org/10.3390/antibiotics10040402>.
- Molino, A., Larocca, V., Chianese, S., Musmarra, D., 2018. Biofuels Production by Biomass Gasification: a Review. *Energies (basel)* 11, 811. <https://doi.org/10.3390/en11040811>.
- Osman, A.I., Fawzy, S., Farghali, M., El-Azazy, M., Elgarahy, A.M., Fahim, R.A., Maksoud, M.I.A.A., Ajlan, A.A., Youstry, M., Saleem, Y., Rooney, D.W., 2022. Biochar for agronomy, animal farming, anaerobic digestion, composting, water treatment, soil remediation, construction, energy storage, and carbon sequestration: a review. *Environ. Chem. Lett.* 20, 2385–2485. <https://doi.org/10.1007/s10311-022-01424-x>.
- Pandey, D.S., Kwapinska, M., Gómez-Barea, A., Horvat, A., Fryda, L.E., Rabou, L.P.L.M., Leahy, J.J., Kwapinski, W., 2016. Poultry Litter Gasification in a Fluidized Bed Reactor: Effects of Gasifying Agent and Limestone Addition. *Energy Fuel* 30, 3085–3096. <https://doi.org/10.1021/acs.energyfuels.6b00058>.
- Pinto, F., André, R., Miranda, M., Neves, D., Varela, F., Santos, J., 2016. Effect of gasification agent on co-gasification of rice production wastes mixtures. *Fuel* 180, 407–416. <https://doi.org/10.1016/j.fuel.2016.04.048>.
- Polish Council of Ministers, 2020. Polish Council of Ministers (Poland), Warsaw.
- Poornima, S., Manikandan, S., Prakash, R., Deena, S.R., Subbaiya, R., Karmegam, N., Kim, W., Govarthanan, M., 2024. Biofuel and biochemical production through biomass transformation using advanced thermochemical and biochemical processes – a review. *Fuel* 372, 132204. <https://doi.org/10.1016/j.fuel.2024.132204>.
- Scala, F., 2011. Fluidized-Bed Combustion of Single Coal Char Particles: an Analysis of the burning Rate and of the Primary CO/CO₂ Ratio. *Energy Fuel* 25, 1051–1059. <https://doi.org/10.1021/ef101182s>.
- Selim, O.M., Amano, R.S., 2021. Co-Pyrolysis of Chicken and Cow Manure. *J. Energy Res. Technol.* 143. <https://doi.org/10.1115/1.4047597>.
- Selim, O.M., Hussein, M.S., Amano, R.S., 2020. Effect of heating Rate on Chemical Kinetics of Chicken Manure with Different Gas Agents. *J. Energy Res. Technol.* 142. <https://doi.org/10.1115/1.4047018>.
- Sikarwar, V.S., Zhao, M., Clough, P., Yao, J., Zhong, X., Memon, M.Z., Shah, N., Anthony, E.J., Fennell, P.S., 2016. An overview of advances in biomass gasification. *Energy Environ. Sci.* 9, 2939–2977. <https://doi.org/10.1039/C6EE00935B>.
- Song, H., Yang, G., Xue, P., Li, Y., Zou, J., Wang, S., Yang, H., Chen, H., 2022. Recent development of biomass gasification for H₂ rich gas production. *Appl. Energy Combust. Sci.* 10, 100059. <https://doi.org/10.1016/j.jaecs.2022.100059>.
- Taifouris, M., Martín, M., 2023. Towards energy security by promoting circular economy: a holistic approach. *Appl. Energy* 333, 120544. <https://doi.org/10.1016/j.apenergy.2022.120544>.
- Tang, F., Zhu, Z., Xu, C., Chi, Y., Jin, Y., 2023. Effects of steam and CO₂ on gasification tar composition and evolution of aromatic compounds. *Waste Manag.* 157, 219–228. <https://doi.org/10.1016/j.wasman.2022.12.019>.
- Turzyński, T., Kluska, J., Kardaś, D., 2022. Study on chicken manure combustion and heat production in terms of thermal self-sufficiency of a poultry farm. *Renew. Energy* 191, 84–91. <https://doi.org/10.1016/j.renene.2022.04.034>.
- Wang, M., Yuan, X., Zhu, C., Lu, H., Han, J., Ji, R., Cheng, H., Xue, J., Zhou, D., 2024. Sequential carbonization of pig manure biogas residue into engineered biochar for diethyl phthalate removal toward environmental sustainability. *Waste Manag.* 190, 45–53. <https://doi.org/10.1016/j.wasman.2024.09.005>.
- Wang, Y., Akdeniz, N., 2023. Co-composting poultry carcasses with wood-based, distillers' grain and cow manure biochar to increase core compost temperatures and reduce leachate's COD. *Waste Manag.* 161, 84–91. <https://doi.org/10.1016/j.wasman.2023.02.024>.
- Wu, R., Beutler, J., Baxter, L.L., 2023. Biomass char gasification kinetic rates compared to data, including ash effects. *Energy* 266, 126392. <https://doi.org/10.1016/j.energy.2022.126392>.
- Xue, J., Dong, Z., Chen, H., Zhang, M., Zhao, Y., Chen, Y., Chen, S., 2024. Gasification of the Char Residues with High Ash Content by Carbon Dioxide. *Energies (basel)* 17, 4432. <https://doi.org/10.3390/en17174432>.
- Yuan, X., He, T., Cao, H., Yuan, Q., 2017. Cattle manure pyrolysis process: Kinetic and thermodynamic analysis with isoconversional methods. *Renew. Energy* 107, 489–496. <https://doi.org/10.1016/j.renene.2017.02.026>.
- Zhao, F., Li, D., Chen, H., Zeng, X., Lin, L., Yuan, H., Shan, R., Chen, Y., 2025. Pyrolysis of pig waste from intensive farming operations: Kinetics, product distribution, and transformation of endogenous heavy metals. *J. Hazard. Mater.* 491, 137916. <https://doi.org/10.1016/j.jhazmat.2025.137916>.
- Zhu, G., Huang, J., Wan, Z., Ling, H., Xu, Q., 2022. Cow Dung Gasification Process for Hydrogen Production using Water Vapor as Gasification Agent. *Processes* 10, 1257. <https://doi.org/10.3390/pr10071257>.